

## $\sigma$ -Dative and $\pi$ -Backdative Phenyl Cation–Dinitrogen Interactions and Opposing Sign Reaction Constants in Dual Substituent Parameter Relations<sup>†</sup>

Rainer Glaser,<sup>\*,‡</sup> Christopher J. Horan,<sup>‡</sup> Michael Lewis,<sup>‡</sup> and Heinrich Zollinger<sup>\*,§</sup>

Department of Chemistry, University of Missouri–Columbia, Columbia, Missouri 65211, and  
Technisch-Chemisches Laboratorium, Eidgenössische Technische Hochschule,  
CH-8092 Zürich, Switzerland

Received September 9, 1998

For the overwhelming number of reactions studied with dual substituent parameter treatments, the ratio of the reaction constants  $\rho_R/\rho_F = \lambda$  is positive and close to unity. Dediazoniations are prominent representatives of the very few unusual reactions for which dual substituent parameter (DSP) relations yield reaction constants of opposing sign. To understand this exceptional behavior, we have studied with *ab initio* methods the energetic, structural, and electronic relaxations along the unimolecular, linear dediazonation path of benzenediazonium ions X-1 to form phenyl cation X-2 in detail for the parent system and two important derivatives (X = H, NH<sub>2</sub>, NO<sub>2</sub>). The results support the electron density based model that describes CN bonding in X-1 by synergistic  $\sigma$ -dative N → C and C → N  $\pi$ -backdative bonding. The analysis provides a theoretical basis for the interpretation of the opposing sign DSP relationship and, in addition, furnishes details about the electronic structure that cannot be deduced from physical-organic studies alone. Polarizations in the  $\sigma$ -frames critically affect structures (*Q* values) and electronic structures (populations), and consistent explanations of structural and energetic relaxations in the course of the dediazonation reactions require their explicit consideration. The classical tool of  $\pi$ -electron pushing does not suffice to provide a correct account of the electronic structures. In particular, the analysis resolves the apparent paradox that the amino group can function as an electron donor even though it is negatively charged. If  $\sigma$ -polarizations dominate in cases where they counteract  $\pi$ -effects, it would seem reasonable to assume that they also are of comparable magnitude where  $\sigma$ - and  $\pi$ -effects act in concert. In the later case, explanations based on  $\pi$ -polarizations might therefore seem consistent but they might lack a physical basis.

### Introduction

We have been interested in deamination reactions and their relation to modifications of DNA. Small aliphatic and aromatic diazonium ions can play a role in DNA alkylation. Diazonium ions also are important intermediates in deaminations of the amino groups in nucleobases.<sup>1</sup> In this context, we have been studying diazonium ions with physical and theoretical organic methods. We proposed a new bonding model for diazonium ions which emphasizes dative bonding of an overall nearly neutral N<sub>2</sub> group to a carbenium ion.<sup>2</sup> Only in heterosubstituted diazonium ions is the charge actually associated with the diazo group.<sup>3</sup> The significance of any bonding model is judged by its ability to explain experimental observation consistently and better than alternative models. We

provided experimental support for this electron density based<sup>4</sup> bonding model via analyses of the first crystal structures of aliphatic diazonium ions,<sup>5</sup> and studies of “incipient nucleophilic attack” established a further link to experiment.<sup>6</sup> More recently, we reported on our studies of the dediazonation of benzenediazonium ion, H-1, to form phenyl cation, H-2.<sup>7</sup> Aryl cations<sup>8</sup> were first generated<sup>9,10,11</sup> by unimolecular dediazonation of benzenediazonium ions, and the elucidation of the details of this mechanism remain a matter of research today.<sup>12</sup> The stationary structures of H-1 were characterized, and

(4) The term “electron density based bonding model” is used to indicate that the model is derived by analysis of the electron density distribution of the unperturbed molecule. Such bonding models have to be distinguished from bonding models that are based on reactivities. Reactivity based bonding models reflect inductive effects while electron density based models do not.

(5) (a) Glaser, R.; Chen, G. S.; Barnes, C. L. *Angew. Chem., Int. Ed. Engl.* **1992**, *31*, 740. (b) Chen, G. S.; Glaser, R.; Barnes, C. L. *J. Chem. Soc., Chem. Commun.* **1993**, 1530.

(6) Glaser, R.; Horan, C. J. *Can. J. Chem.* **1996**, *74*, 1200 and references cited therein.

(7) Glaser, R.; Horan, C. J. *J. Org. Chem.* **1995**, *60*, 7518.

(8) For recent reviews of aryl cations, see: *Dicoordinated Carbocations*; Rappoport, Z., Stang, P. J., Eds.; An Interscience Publication, John Wiley & Sons: Chichester, 1997; Chapters 4 and 10

(9) Zollinger, H. *Angew. Chem., Int. Ed. Engl.* **1978**, *17*, 141 and references cited therein.

(10) Swain, C. G.; Sheats, J. E.; Harbison, K. G. *J. Am. Chem. Soc.* **1975**, *97*, 783.

(11) Lewis, E. S.; Hartung, L. D.; McKay, B. M. *J. Am. Chem. Soc.* **1969**, *91*, 419 and references cited therein.

(12) Garcia-Mejide, M. C.; Bravo-Diaz, C.; Romsted, L. S. *Int. J. Chem. Kinet.* **1998**, *30*, 31 and references cited therein.

\*To whom correspondence should be addressed. R.G.: facsimile, (573) 882-2754; E-mail, GlaserR@missouri.edu. H.Z.: telephone, (41) 1 910-5308; facsimile, (41) 1 632-1072.

<sup>†</sup>Presented in part at the 30th Midwest Theoretical Chemistry Conference, University of Illinois, Urbana–Champaign, May 22–24, 1997, and in the symposium on Electrophilic DNA-Damage, Organic Chemistry Division, 215th National Meeting of the American Chemical Society, Dallas, TX, March 29–April 2, 1998.

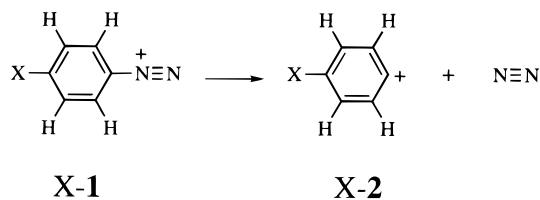
<sup>‡</sup>Department of Chemistry, University of Missouri–Columbia.

<sup>§</sup>Technisch-Chemisches Laboratorium, ETH Zürich.

(1) Glaser, R.; Son, M.-S. *J. Am. Chem. Soc.* **1996**, *118*, 10942 and references cited therein.

(2) Glaser, R.; Choy, G. S.-C.; Hall, M. K. *J. Am. Chem. Soc.* **1991**, *113*, 1109 and references cited therein.

(3) Glaser, R.; Choy, G. S.-C. *J. Am. Chem. Soc.* **1993**, *115*, 2340 and references cited therein.



energies for automerization and unimolecular dissociation were reported at theoretical levels that were shown to reproduce experimental binding energies and solid-state structures very well. Moreover, the study of H-1 allowed for a broad examination of the consistency of the bonding model with a variety of experimental data and the bonding model was found to be general. In going one step further, one can employ the vast experimental data on the kinetics of the dediazoniations of substituted benzenediazonium ions to build a further and compelling link between theoretical electron density analysis and the physical organic chemists' experimental probes for electron density relaxations. This is the topic of the present paper, and as will be seen, the combined analysis offers much greater insights than either method alone.

### Hammett Equation and Dual Substituent Parameter Treatments

Dediazoniations cannot be described by the Hammett equation<sup>13</sup> (eq 1) but require instead a dual substituent parameter (DSP) treatment in which resonance (mesomeric) and field (inductive) resonance constants of *opposing* signs are used.<sup>14a</sup> Use of the Taft equation<sup>15</sup> (eq 2) provides good correlations with experimental rate constants. Taft analysis results in reaction

$$\log(k_X/k_0) = \sigma\rho \quad (1)$$

$$\log(k_X/k_0) = \sigma_F\rho_F + \sigma_R\rho_R \quad (2)$$

$$\log(k_X/k_0) = (\text{polarity})\rho_F + (\text{charge transfer})\rho_R \quad (3)$$

constants that differ greatly in magnitude and have opposite signs  $\rho_F < -3.5$  and  $\rho_R > +2.2$ . Topsom<sup>16a</sup> classified electronic substituent actions into effects that are associated with the substituent's polarity ( $\sigma$ -inductive effect  $I$ , field effect  $F$ ,  $\sigma$ -induced  $\pi$ -effect  $\pi_s$ , field-induced  $\pi$ -effect  $\pi_F$ ) and effects that are assigned to the substituent's charge-transfer ability (mesomeric effect  $R$ ,  $\pi$ -induced  $\sigma$ -effect  $\sigma_\pi$ ). This classification relates the substituent constants  $\sigma_F$  and  $\sigma_R$  in eq 2 to polarity and charge-transfer factors as indicated by eq 3. In subsequent theoretical studies, Topsom<sup>16b,c</sup> reduced electronic effects into four inherent effects that describe the field effects ( $\sigma_F$ ), the electronegativity effects ( $\sigma_X$ ), the polarizability effects ( $\sigma_a$ ), and resonance effects (R). The substituent constants in the Hammett equation are assumed to be

characteristic of the substituent and independent of the reaction. Streitwieser et al. showed that this is indeed the case for most substituents.<sup>17</sup> In that article, Streitwieser also pointed out that "the actual mechanism by which a substituent modifies chemical reactivity has yet to be described" and this remains true to date for aromatic systems. Dual substituent parameter treatments can thus be seen as the necessary consequence of the two classes of intrinsic substituent effects.<sup>18</sup> Interestingly, experience shows that in the great majority of reactions the ratio  $\rho_R/\rho_F = \lambda \approx 1$ . It is for this reason that the Hammett  $\sigma\rho$  relation has been fairly well applicable to several thousand heterolytic reactions of substituted benzene derivatives.<sup>19</sup> We estimate that values of  $\lambda$  larger than 1.1 or smaller than 0.9 (but still positive) are present in fewer than 10% of all equilibria. This result seems surprising as the field effect and resonance effect are, in principle, considered to be independent of each other and there is no obvious reason both effects should affect the reactivity in the same direction and to the same relative extent. Among the thousands of reactions studied, only *very few* reactions are known with opposing signs of field and resonance reaction constants  $\rho_F$  and  $\rho_R$ . The 16 reactions were summarized by Zollinger,<sup>14a</sup> and they include the dediazoniations of aryldiazonium ions in water, in 1,2-dichloroethane,<sup>14b</sup> and in trifluoroethanol.<sup>14c</sup> The DSP analysis for the automerization of benzenediazonium ion results in reaction constants ( $\rho_F = -3.4$  and  $\rho_R = 2.5$ ) that agree closely with the respective values for the dediazoniations.<sup>3a</sup> Zollinger interpreted the opposing signs of the reaction constants  $\rho_F$  and  $\rho_R$  in the Taft DSP treatments by surmising that  $\sigma$ -dative C–N bonding is accompanied by C  $\rightarrow$  N  $\pi$ -backdative bonding. While this interpretation cannot be demonstrated experimentally, it is possible to scrutinize this hypothesis with electronic structure methods, and electron density analysis of the unimolecular dissociations X-1  $\rightarrow$  X-2 + N<sub>2</sub> have been carried out to do so. Here we report an analysis of the energetic, structural, and electronic relaxation along the dissociation path of H-1 and its *para*-substituted derivatives NH<sub>2</sub>-1 and NO<sub>2</sub>-1.<sup>20</sup> Our objectives are (a) to show that the reaction constants of the dediazonation reactions are consistent with the C–N  $\sigma$ -dative/C  $\rightarrow$  N  $\pi$ -backdative bonding hypothesis and (b) to learn about the actual mechanisms by which two important substituents (NH<sub>2</sub>  $\sigma_p$   $-0.66$ ,  $\sigma_F$   $+0.08$ ,  $\sigma_R$   $-0.74$ ; NO<sub>2</sub>  $\sigma_p$   $+0.78$ ,  $\sigma_F$   $+0.65$ ,  $\sigma_R$   $+0.13$ ) do affect electronic structure. The electron density analysis is based on the topological features of the *total* electron density which is an "observable". We also determined the  $\sigma$ - and  $\pi$ -components of the atom populations. While these components are not "observable" in the strict quantum-mechanical sense, the concept of  $\sigma/\pi$  separation is a successful one and it is central to all models invoking

(13) (a) Hammett, L. P. *Chem. Rev.* **1935**, *17*, 125. (b) Hammett, L. P. *J. Am. Chem. Soc.* **1937**, *59*, 96. (c) Hammett, L. P. *Faraday Soc. Trans.* **1938**, *341*, 156. (d) Jaffe, H. H. *Chem. Rev.* **1953**, *53*, 191.

(14) (a) Zollinger, H. *J. Org. Chem.* **1990**, *55*, 3846. (b) Nakazumi, H.; Kitao, T.; Zollinger, H. *J. Org. Chem.* **1987**, *52*, 2825. (c) Ravenscroft, M. D.; Zollinger, H. *Helv. Chim. Acta* **1988**, *71*, 507. (d) Zollinger, H. *Diazo Chemistry I*; VCH Publishers: New York, 1994.

(15) (a) Taft, R. W.; Deno, N. C.; Skell, P. P. *Annu. Rev. Phys. Chem.* **1958**, *9*, 287. (b) Taft, R. W.; Lewis, I. C. *J. Am. Chem. Soc.* **1958**, *80*, 2436. (c) Taft, R. W. *J. Phys. Chem.* **1960**, *64*, 1805.

(16) (a) Topsom, R. D. *Prog. Phys. Org. Chem.* **1976**, *12*, 1. (b) Taft, R. W.; Topsom, R. D. *Prog. Phys. Org. Chem.* **1987**, *16*, 1. (c) Topsom, R. D. *Prog. Phys. Org. Chem.* **1987**, *16*, 125.

(17) (a) Vorpapel, E. R.; Streitwieser, A.; Alexandratos, S. D. *J. Am. Chem. Soc.* **1981**, *103*, 3777. (b) Niwa, J. *Bull. Chem. Soc. Jpn.* **1989**, *62*, 226.

(18) For a survey of Hammett substituent constants and resonance and field parameters, see: Hansch, C.; Leo, A.; Taft, R. W. *Chem. Rev.* **1991**, *91*, 165.

(19) (a) Hansch, C.; Leo, A. *Exploring QSAR—Fundamentals and Applications in Chemistry and Biology*, ACS Professional Reference Book; American Chemical Society: Washington, DC, 1995. (b) Hansch, C.; Leo, A.; Hoekman, D. *Exploring QSAR—Hydrophobic, Electronic, and Steric Constants*, ACS Professional Reference Book; American Chemical Society: Washington, DC, 1995.

(20) Communicated in part: Glaser, R.; Horan, C. J.; Zollinger, H. *Angew. Chem., Int. Ed. Engl.* **1997**, *36*, 2210.

dative and backdative bonding. In essence, our analysis links electron density shifts in the  $\sigma$ - and  $\pi$ -systems with the reaction constants  $\rho_F$  and  $\rho_R$  and we note that this approach differs slightly from Topsom's *ansatz* in that we would weight  $\pi_S$  and  $\pi_F$  terms  $\rho_R$ . Ideally, an analysis of this relatively clear and qualitatively explainable case of a reaction with opposing field and resonance effects may lead to an understanding as to why thousands of equilibria and reactions follow the Hammett equation with an almost constant ratio of the two effects, as shown by  $1.1 > \lambda > 0.9$ .

### Electronic Structure Theoretical Methods and Computations

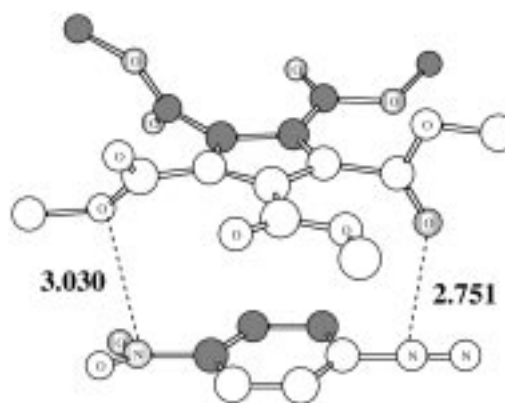
*Ab initio* calculations were carried out with Gaussian94<sup>21,22</sup> and earlier versions on IBM RS-6000 and Silicon Graphics Indigo workstations. Unless otherwise stated, geometries were optimized within the constraints imposed by  $C_{2v}$  symmetry. Structures of X-1 and X-2 along the dissociation path were optimized in  $C_{2v}$  symmetry with the appropriate constraint on the C–N bond. Vibrational analyses were performed for stationary structures to obtain harmonic vibrational frequencies and zero-point energies. Optimization and vibrational analyses were carried out at the RHF/6-31G\* level. For H-1 and H-2, we examined electron correlation effects on vibrational frequencies previously. Vibrational zero-point energy corrections to binding energies and activation barriers were scaled by factors 0.9135 (RHF/6-31G\*) and 0.9646 (MP2/6-31G\*).<sup>23</sup> The energy profiles for the dissociations of X-1 (X = H, NH<sub>2</sub>, NO<sub>2</sub>) were determined on the basis of RHF/6-31G\* structures. The effects of electron correlation on the energy profile were examined for H-1 at the levels MP2(fc)/6-31G\*\*/RHF/6-31G\* and MP3(fc)/6-31G\*\*/RHF/6-31G\*. Furthermore, for H-1 the path calculations were carried out using MP2(full)/6-31G\* optimized structures. For all systems, geometries of the stationary structures were refined at the MP2(full)/6-31G\* level and higher level energies were computed at the levels MP3(fc)/6-31G\*, MP4(sdtq,fc), and QCISD-(T,fc)/6-31G\* on the basis of the MP2(full)/6-31G\* structures.

Topological and integrated properties<sup>24,25</sup> were determined with the programs Extreme<sup>26</sup> and Proaim.<sup>27</sup> Electron density analyses were carried out at the level RHF/6-31G\* for stationary structures X-1 and X-2 and the associated dissociation paths for X = H, NH<sub>2</sub>, and

NO<sub>2</sub>. The topological properties of bond and ring critical points of the stationary structures as well as are integrated properties are given in the Supporting Information, and some pertinent data are given in Figures 5–7. For H-1 and H-2, electron density analyses were carried out at the correlated levels MP2(full)/6-31G\* (including dissociation path) and CISD(full)/6-31G\*\*/RHF/6-31G\* as well, and the corresponding topological and integrated properties also can be found in the Supporting Information. The study of the theoretical level dependency confirms earlier insights<sup>3</sup> and further justifies our choice of theoretical level.

### Results and Discussion

**Potential Energy Surface of Benzenediazonium Ions and Binding Energies.** We presented a potential energy surface analysis of H-1 earlier and revised the previously described PES characteristics.<sup>28</sup> The geometry of PhN<sub>2</sub><sup>+</sup> with a linear  $C_{\text{ipso}}\text{-N}\equiv\text{N}$  skeleton, H-1, was compared to the solid-state structures of the salts<sup>29</sup> PhN<sub>2</sub><sup>+</sup>X<sup>-</sup> (with X<sup>-</sup> = Cl<sup>-</sup>, Br<sub>3</sub><sup>-</sup>, BF<sub>4</sub><sup>-</sup>), and the agreement between theory and experiment was found to be excellent. End-on coordination is greatly preferred over  $\eta^2$ -bridged structures, and only the former is considered here. We have now carried out a detailed study of the unimolecular reaction X-1  $\rightarrow$  X-2 with consideration of several structures along the linear C–N dissociation path for the parent system X = H and for the *p*-amino- and *p*-nitro-substituted systems. Molecular models of stationary structures are shown in Figure 1, and the potential energy profiles of the unimolecular dissociation reactions 1  $\rightarrow$  2 for X = H, NH<sub>2</sub>, and NO<sub>2</sub> are shown in Figures 2 and 3. The computed structure of NO<sub>2</sub>-1 can be compared to the crystal structure of its salt O<sub>2</sub>NPhN<sub>2</sub><sup>+</sup>BF<sub>4</sub><sup>-</sup>.<sup>30a</sup> Note that the structure of the salt<sup>30b</sup> of O<sub>2</sub>NPhN<sub>2</sub><sup>+</sup>[Cp(CO<sub>2</sub>Me)<sub>5</sub>]<sup>-</sup> does *not* provide a suitable reference since strong inter-



molecular interactions occur that are reminiscent of incipient nucleophilic attack.<sup>6</sup> The ion NH<sub>2</sub>-1 has not been

(21) Gaussian94, Revision C.3: Frisch, M. J.; Trucks, G. W.; Schlegel, H. B.; Gill, P. M. W.; Johnson, B. G.; Robb, M. A.; Cheeseman, J. R.; Keith, T.; Petersson, G. A.; Montgomery, J. A.; Raghavachari, K.; Al-Laham, M. A.; Zakrzewski, V. G.; Ortiz, J. V.; Foresman, J. B.; Cioslowski, J.; Stefanov, B. B.; Nanayakkara, A.; Challacombe, M.; Peng, C. Y.; Ayala, P. Y.; Chen, W.; Wong, M. W.; Andres, J. L.; Replogle, E. S.; Gomperts, R.; Martin, R. L.; Fox, D. J.; Binkley, J. S.; Defrees, D. J.; Baker, J.; Stewart, J. J. P.; Head-Gordon, M.; Gonzalez, C.; Pople, J. A. Gaussian, Inc., Pittsburgh, PA, 1995.

(22) Hehre, W. J.; Radom, L.; Schleyer, P. v. R.; Pople, J. A. *Ab Initio Molecular Orbital Theory*; John Wiley & Sons: New York, 1986.

(23) Pople, J. A.; Scott, A. P.; Wong, M. W.; Radom, L. *Isr. J. Chem.* **1993**, *33*, 345.

(24) Bader, R. F. W. *Atoms in Molecules, A Quantum Theory*; Oxford Science Publications: Clarendon Press: Oxford, 1990.

(25) Biegler-König, F. W.; Bader, R. W.; Tang, T.-H. *J. Comput. Chem.* **1982**, *3*, 317.

(26) Biegler-König, F. W., McMaster University, Hamilton, ON, Canada, 1980.

(27) (a) Biegler-König, F. W.; Duke, F. A., McMaster University, Hamilton, ON, Canada, 1981. (b) Modifications by Lau, C. D. H., McMaster University, Hamilton, ON, Canada, 1983.

(28) (a) Dill, J. D.; Schleyer, P. v. R.; Pople, J. A. *J. Am. Chem. Soc.* **1977**, *99*, 1. (b) Alcock, N. W.; Greenhough, T. V.; Hirst, D. M.; Kemp, T. J.; Payne, D. R. *J. Chem. Soc., Perkin Trans. 2* **1980**, *1*, 8. (c) Vincent, M. A.; Radom, L. *J. Am. Chem. Soc.* **1978**, *100*, 3306.

(29) (a) Rømming, C. *Acta Chem. Scand.* **1963**, *17*, 1444. (b) Andresen, O.; Rømming, C. *Acta Chem. Scand.* **1962**, *16*, 1882. (c) Cygler, M.; Przybylska, M.; Eloffson, R. *Can. J. Chem.* **1982**, *60*, 2852.

(30) (a) *p*-Nitrobenzenediazonium tetrafluoroborate: Barnes, J. C.; Butler, A.; Anderson, L. *Acta Crystallogr. C* **1990**, *46*, 945. (b) 4-Nitrobenzenediazonium pentamethylcyclopentadienide-1,2,3,4,5-pentacarboxylate: Kompan, O. E.; Antipin, M. Y.; Struchkov, Y. T.; Mikhailov, I. E.; Dushenko, G. A.; Olekhovich, L. P.; Minkin, V. I. *Zh. Org. Khim.* **1985**, *21*, 2032.

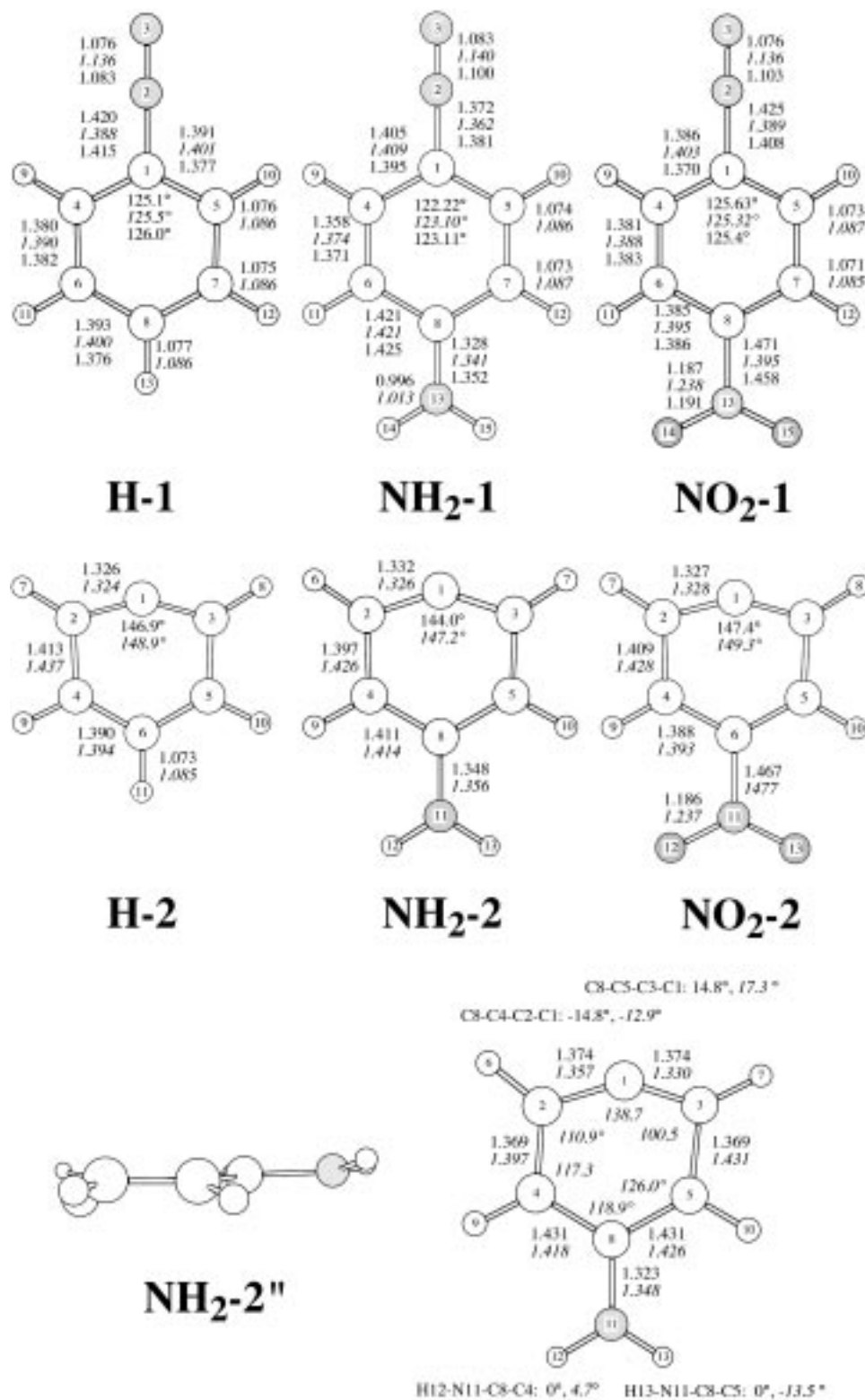


**Figure 1.** Molecular models of the benzenediazonium ions X-1 (X = H, NH<sub>2</sub>, NO<sub>2</sub>) and of the phenyl cations X-2 as determined at the levels RHF/6-31G\* and MP2(full)/6-31G\* (in italics). For the diazonium ions, the experimental values derived from the X-ray crystallographic analysis of the tetrafluoroborate salts are given as well (third value given).

prepared to date but solid-state structures are available for two salts containing dialkylamino derivatives R<sub>2</sub>NPhN<sub>2</sub><sup>+</sup> (with anions BF<sub>4</sub><sup>-</sup> or ZnCl<sub>4</sub><sup>2-</sup>)<sup>31</sup> The structure of Me<sub>2</sub>N-1 in the zincate differs greatly from the computed structure with respect to the  $\angle$ (C–C<sub>ipso</sub>–C) (130.2°) and the C<sub>ipso</sub>–N<sub>2</sub> bond length (1.479 Å). Neither of the

structures exhibit significant specific cation–anion interactions, and it is likely that the accuracy of the zincate structure<sup>31b</sup> does not meet modern standards. Hence, we provide in Figure 1 the experimental data for the tetrafluoroborates of all three diazonium ions. The binding energies,  $E_b$ , are the reaction energies for the dis-

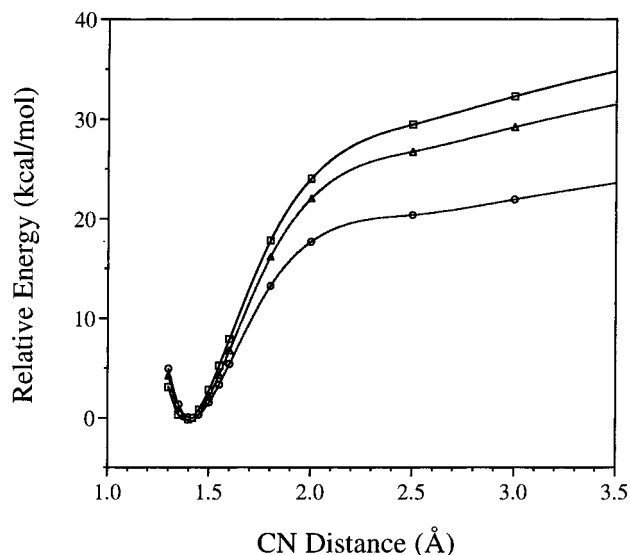


**Figure 2.** Potential energy profile of the linear dediazonation path of H-1 determined at the levels RHF/6-31G\* (circles), MP2(fc)/6-31G\*\*/RHF/6-31G\* (squares), and MP3(fc)/6-31G\*\*/RHF/6-31G\* (triangles).

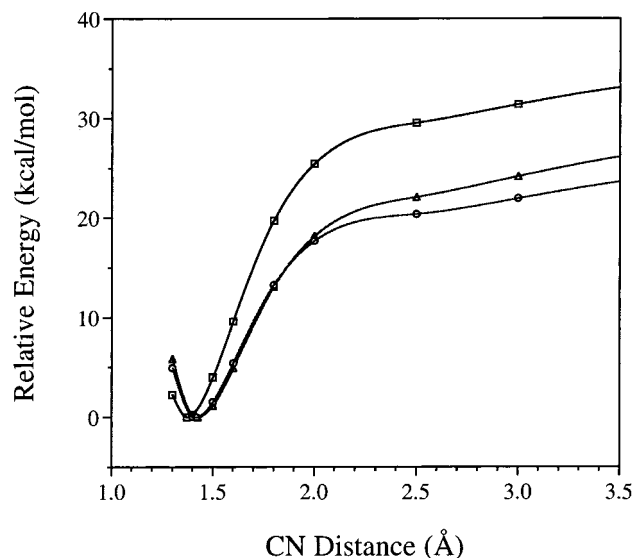


**Figure 3.** Potential energy profiles of the linear dediazonation paths of X-1 for X = H (circles), X = NH<sub>2</sub> (squares), and X = NO<sub>2</sub> (triangles) at the RHF/6-31G\* level.

sociation of X-1 to form phenyl cation X-2 and N<sub>2</sub> which is the reaction channel with the lowest activation barrier,<sup>32</sup> and the computed binding energies are collected in Table 1.

The C<sub>2v</sub> structures X-1 are minima, and H-2 and NO<sub>2</sub>-2 also prefer C<sub>2v</sub> symmetry. Unexpectedly, however, the RHF/6-31G\* C<sub>2v</sub> structure NH<sub>2</sub>-2 is not a minimum but a second-order saddle point (i242 (b<sub>1</sub>) and i120 (b<sub>1</sub>) cm<sup>-1</sup>). The displacement vectors associated with the i120 (b<sub>1</sub>) cm<sup>-1</sup> mode correspond to amino-N pyramidalization. The

major distortion indicated by the other imaginary mode consists of a motion of C<sub>ipso</sub> out of plane and is accompanied by motion of the o-CH groups onto the opposite side of the plane. Reoptimization of NH<sub>2</sub>-2 without symmetry constraints and a small symmetric oop distortion of the amino hydrogens resulted in a structure with *de facto* C<sub>s</sub> symmetry and a minor amino group pyramidalization (NH<sub>2</sub>-2'). This structure is a transition state structure (i229, a'), and the imaginary mode indicates a distortion at C<sub>ipso</sub> as discussed for NH<sub>2</sub>-2. The minimum energy structure NH<sub>2</sub>-2'' was located starting with a more strongly distorted trial structure and optimization without any symmetry constraints. The result was a *de facto* C<sub>s</sub> symmetric structure NH<sub>2</sub>-2'' structure in which C<sub>ipso</sub> was markedly moved out of the best molecular plane. Note that the amino N in the solid-state structure of 4-morpholinobenzenediazonium also is pyramidal.<sup>31a</sup> While it is well-known that aniline<sup>33</sup> contains a nonplanar amino group, the nonplanarity of the amino group in the phenyl cation is expected even less. NH<sub>2</sub>-2' is basically isoenergetic with the C<sub>2v</sub> structure, and even NH<sub>2</sub>-2'' is only 1.22 kcal/mol more stable. Optimization of NH<sub>2</sub>-2'' at MP2(full)/6-31G\* resulted in a chiral minimum structure, and a molecular model of this structure is shown in Figure 1. The major advantage of NH<sub>2</sub>-2'' appears to be the release of ring strain at C<sub>ipso</sub>. At the MP2(full)/6-31G\* level, NH<sub>2</sub>-2'' is only 1.61 kcal/mol more stable as compared to NH<sub>2</sub>-2. The vibrational zero-point energy difference between NH<sub>2</sub>-2 and NH<sub>2</sub>-2'' is of about the same magnitude, and the energetic benefit due to the distortions is rather small. These distortions do not play a role until the very late stages of unimolecular dissociation. While we do report the binding energies in Table 1 with respect to NH<sub>2</sub>-2'', we are considering NH<sub>2</sub>-2 in all other instances.

In Figure 2, the theoretical level dependency of the energy profiles are shown for H-1. The shapes of the profiles are qualitatively the same while there are quantitative differences. Systematic studies of the theoretical model dependency of the binding energies of XN<sub>2</sub><sup>+</sup> systems have shown that binding energies computed at the MP3 level and including vibrational zero-point energies reproduce experimental gas phase binding energies sufficiently accurately. At the MP3//RHF+ΔVZPE-(RHF)<sub>scaled</sub> level, we find E<sub>b</sub>(H-2) = 28.7 kcal/mol which is very close to the value of 27.5 kcal/mol determined at QCISD(T)//MP2+ΔVZPE(RHF)<sub>scaled</sub>. Kuokkanen reported an activation energy for the dissociation of H-1 in dichloroethane of 25.8 kcal/mol.<sup>34</sup> Zollinger *et al.* studied the decomposition of H-1 in 2,2,2-trifluoroethanol in the presence or absence of benzene and determined activation energies of 27.7 and 28.3 kcal/mol, respectively.<sup>35</sup> The good agreement between the calculated gas phase and the measured solution data suggests that it is also primarily the intrinsic properties of the benzenediazonium ion that are reflected in the solution chemistry.

The binding energies of NH<sub>2</sub>-2 and of NO<sub>2</sub>-2 both are higher than the one for H-2. This is true at all levels (Table 1) and the potential energy profiles are compared

(31) (a) 4-Morpholinobenzenediazonium tetrafluoroborate: Alcock, N. W.; Greenhough, T. J.; Hirst, D. M.; Kemp, T. J.; Payne, D. R. *J. Chem. Soc., Perkin Trans. 2* **1980**, 8. (b) *p*-(*N,N*-Dimethylamino)-phenyldiazonium chlorozincate: Nesterova, Y. M.; Porai-Koshits, M. A. *Zh. Strukt. Khim.* **1971**, 12, 108.

(32) (a) Bergstrom, R. G.; Landells, R. G. M.; Wahl, G. H., Jr.; Zollinger, H. *J. Am. Chem. Soc.* **1976**, 98, 3301. (b) Swain, C. G.; Sheats, J. E.; Harbison, K. G. *J. Am. Chem. Soc.* **1975**, 97, 783.

(33) (a) Jiang, J. C.; Lin, C. E. *Theochem* **1997**, 392, 181. (b) Bludsky, O.; Sponer, J.; Leszczynski, J.; Spirko, V.; Hobza, P. *J. Chem. Phys.* **1996**, 105, 11042.

(34) (a) Kuokkanen, T.; Virtanen, P. O. I. *Acta Chem. Scand. B* **1979**, 33, 725. (b) Kuokkanen, T. *Acta Chem. Scand.* **1990**, 44, 394.

(35) Burri, P.; Wahl, G. H., Jr.; Zollinger, H. *Helv. Chim. Acta* **1974**, 57, 2099.

**Table 1. Binding Energies and Vibrational Zero-Point Corrections**

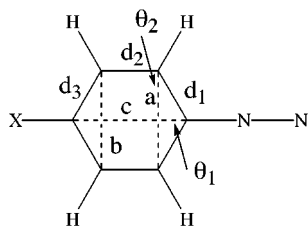
reaction	RHF//RHF	$\Delta$ VZPE	MP2//MP2	MP3(fc)//MP2	MP4(fc)//MP2	QCISD(T)//MP2
H-1 $\rightarrow$ H-2 + N <sub>2</sub>	25.61	-4.71	38.64	33.43	34.28	32.20
NH <sub>2</sub> -1 $\rightarrow$ NH <sub>2</sub> -2 (C <sub>1</sub> ) + N <sub>2</sub>	33.72	-4.55	47.71	42.52	42.48	39.57
NO <sub>2</sub> -1 $\rightarrow$ NO <sub>2</sub> -2 + N <sub>2</sub>	28.38	-4.61	43.02	36.99	38.39	36.05

<sup>a</sup> All calculations employ the 6-31G\* basis set. <sup>b</sup> The vibrational zero-point energy corrections need to be added to the reaction energies to obtain approximate reaction enthalpies,  $\Delta H = \Delta E + \Delta$ VZPE.

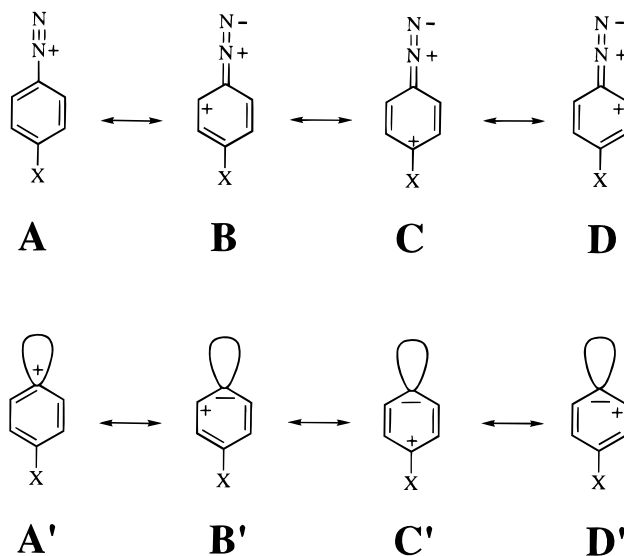
in Figure 3. At our highest computational level, QCISD-(T)/6-31G\*//MP2(full)/6-31G\* +  $\Delta$ VZPE(MP2(full)/6-31G\*), we find binding energies of 27.5 (X = H), 35.0 (X = NH<sub>2</sub>), and 31.4 kcal/mol (X = NO<sub>2</sub>). The  $\Delta$ VZPE values are rather similar for all X, and the differences in the binding energies thus are reflective of electronic differences. Both the NH<sub>2</sub> and the NO<sub>2</sub> groups are overall electron-withdrawing groups, and they are expected to destabilize the phenyl cation with its electron deficiency in the  $\sigma$ -system more than they destabilize the corresponding diazonium ion. But why is the dissociation of NH<sub>2</sub>-1 more endothermic than that of NO<sub>2</sub>-1? One might expect the opposite since the nitro group is more electron-withdrawing and, in addition, because the  $\pi$ -donor might better compensate the electron deficiency in the  $\sigma$ -frame via polarization of the  $\pi$ -system. Qualitative considerations of X-2 thus would suggest just the opposite to the finding  $E_b(\text{NH}_2\text{-2}) > E_b(\text{NO}_2\text{-2})$ , and they point out that there must exist significant differences in the electronic structures of NH<sub>2</sub>-1 and NO<sub>2</sub>-1 which provide an extra stabilization to NH<sub>2</sub>-1.

Electron correlation effects are important to reproduce the potential energy profiles of the dissociation in a near-quantitative fashion. But the data in Table 1 and Figures 2 and 3 show that the RHF results do allow for qualitatively correct descriptions of the heterolyses. In light of the high computational demand, the topological electron density analyses of the dissociation paths of X-1 were carried out at the RHF/6-31G\* level.

**Structural Relaxation along the Dissociation Path.** The structural differences between H-1 and NO<sub>2</sub>-1 (Figure 1) are minor (within 0.01 Å and 1°) while the effects of a push–pull interaction are clearly manifest in NH<sub>2</sub>-1. The CC bonds in NH<sub>2</sub>-1 alternate by as much as 0.05 Å while such changes are less (0.01–0.02 Å) in H-1 and NO<sub>2</sub>-1. The N<sub>2</sub>-phenyl contact in NH<sub>2</sub>-1 is shorter, and the angle at C<sub>ipso</sub> is less widened. The structural relaxation upon N<sub>2</sub> dissociation is steady for all X, and the major structural consequences are common. The already widened angle  $\theta_1$  at C<sub>ipso</sub> of H-1 (125.1°) increases further along the dissociation path and splays close to the angle in free H-2 (146.9°) at a CN distance of 3.0 Å (146.3°). The  $\theta_2$  angles at C<sub>ortho</sub> decrease steadily



and half as much as the C<sub>ipso</sub> angle widens and, consequently, the phenyl ring deforms such as to decrease the C<sub>ipso</sub>–C<sub>para</sub> distance c. The C<sub>ipso</sub>–C<sub>ortho</sub> bond length d<sub>1</sub> shortens dramatically (0.06–0.08) as the CN distance increases, and there is a smaller increase (0.03–0.05) of

**Scheme 1. Resonance Forms Describing the Polarizations in the  $\pi$ -Systems of Benzenediazonium Ions (A–D) and of Phenyl Cations (A'–D')**

<sup>a</sup> Note that C<sub>ipso</sub> is formally neutral in B'–D' since the positive charge associated with the  $\sigma$ -hole is compensated for by the double occupation of the p-AO at that C-atom.

the C<sub>ortho</sub>–C<sub>meta</sub> bond lengths d<sub>2</sub>. The C<sub>meta</sub>–C<sub>para</sub> bonds d<sub>3</sub> remain relatively constant along the entire dissociation path ( $\pm 0.005$  Å). Note in particular that the C<sub>ortho</sub>–C<sub>meta</sub> bonds d<sub>2</sub> lengthen to such an extent that they exceed the C<sub>meta</sub>–C<sub>para</sub> bonds d<sub>3</sub> while they were always shorter in X-1. As with the diazonium ions, the phenyl cation structures of the parent and the nitro-substituted system are rather similar. Ion NH<sub>2</sub>-2 shows the same types of deformation upon dediazonation. The diazo function is an extremely electron-withdrawing group with a substituent constant of  $\sigma_p^- = 3.36$ . The results of the electron density analysis are fully compatible in that the substituent “-N<sub>2</sub><sup>+</sup>” withdraws virtually a full charge to become overall nearly neutral (*vide infra*). This property suggests contributions by resonance forms B–D (Scheme 1)—if withdrawal of electron density is due to  $\pi$ -interaction—and consequently severely weakened d<sub>1</sub> bonds, moderately weakened d<sub>3</sub> bonds, and strengthened d<sub>2</sub> bonds. To quantify this notion, we define the parameter  $Q = 1000(d_1 + d_3 - 2d_2)$ . Contributions by B–D should manifest themselves in  $Q > 0$ . Substituents in the para position are expected to reinforce this type of deformation no matter whether the group X is a  $\pi$ -donor (push–pull reinforcement) or a  $\pi$ -acceptor (reversed effect on d<sub>1</sub> and d<sub>3</sub> but effects in the same direction nevertheless). Expectations are thus very clearly defined. The Q values

(36) (a) Lewis, E. S.; Johnson, M. D. *J. Am. Chem. Soc.* **1959**, *81*, 2070. (b) Note that the  $\sigma$  values derived from ionization constants of other systems or from rate data vary. In any case, all  $\sigma$  values determined for the diazonium function are larger than 1.8.

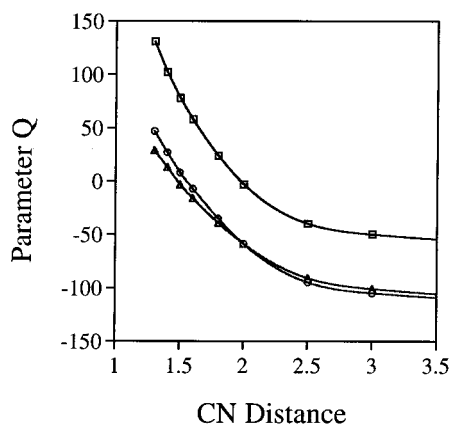


**Figure 4.** The  $Q$  parameter quantifies structural distortions of the benzene rings in the course of C–N cleavage in X-1. Values for X = H (circles), X = NH<sub>2</sub> (squares), and X = NO<sub>2</sub> (triangles) were computed at the level RHF/6-31G\*.

were computed for X-1 as a function of the CN distance, and they are plotted in Figure 4.<sup>37</sup> Positive  $Q$  values are found indeed for the equilibrium structures of the diazonium ions— $Q(\text{H-1}) = 24$  [MP2: 20],  $Q(\text{NH}_2\text{-2}) = 110$  [82], and  $Q(\text{NO}_2\text{-1}) = 9$  [22]—and the magnitude of  $Q$  of NH<sub>2</sub>-2 stands out. More interesting is the behavior of  $Q$  as a function of the CN distance: The  $Q$  values decrease quickly and they become *negative* even before the CN distance exceeds 2 Å. For the phenyl cations, we obtain  $Q(\text{H-2}) = -110$  [MP2: -156],  $Q(\text{NH}_2\text{-2}) = -52$  [-112], and  $Q(\text{NO}_2\text{-2}) = -106$  [-135]. What are the reasons for the negative sign of the  $Q$  values?  $\pi$ -Polarizations in the phenyl cations X-2 do not explain the negative  $Q$  values; they would suggest just the opposite. As the  $\sigma$ -hole develops, the  $\pi$ -system should respond with polarizations of the  $C_{\text{ipso}}\text{--}C_{\text{ortho}}$   $\pi$ -bonds (B' and D') and with secondary polarization (C'). The latter should be important especially for  $\pi$ -donor X groups. Contributions from B'–D' would clearly suggest positive  $Q$  values. The reason for the negative  $Q$  values thus must lie with  $\sigma$ -polarizations. The  $\sigma$ -orbitals of  $C_{\text{ipso}}$  assume as much s character as possible to become more electronegative and to polarize the  $C_{\text{ipso}}\text{--}C_{\text{ortho}}$  bonds.

#### Electronic Structures of Benzenediazonium Ions.

The C–N bonding situations in the aromatic diazonium ions is much the same as in all of the aliphatic diazonium ions studied previously. In general, diazonium ions are best thought of as a carbenium ion closely associated with



an N<sub>2</sub> group that is internally polarized in the fashion N<sub>α</sub><sup>δ-</sup>–N<sub>β</sub><sup>δ+</sup>. Our bonding model implies N → C  $\sigma$ -dative bonding instead of the covalent C–N bond formation and charge transfer formally indicated by Lewis notation. We have shown with a combination of theoretical and experimental methods that the notion of “the carbenium ion within the diazonium ion” is fully warranted irrespective of charge and nature of the R group. The

integrated phenyl charge of H-1 is +0.974. The N<sub>2</sub> group is overall nearly neutral and polarized,  $q(\text{N}_\alpha) = -0.540$  and  $q(\text{N}_\beta) = +0.558$ . The charge distributions in the CN<sub>2</sub> regions of H-1 and NO<sub>2</sub>-1 are similar (Figure 5), and the latter system does show the expected slightly higher positive charge on the diazo group. In NH<sub>2</sub>-1, a charge of the H<sub>2</sub>NC<sub>6</sub>H<sub>4</sub> fragment in excess of +1 and a negatively charged N<sub>2</sub> group occurs as the result of strong C → N  $\pi$ -donation of 0.338 electrons while the Ph → N<sub>2</sub>  $\pi$ -donation is just about half that much in H-1 (0.211) and NO<sub>2</sub>-1 (0.185). For all X-1, the N → C charge transfer via  $\sigma$ -donation is very much the same in that the  $\sigma$ -charge does not vary significantly from 0.231. The charge transfer associated with CN bonding in X-1 can therefore be accurately described by a bonding model that involves N → C  $\sigma$ -donation and C → N  $\pi$ -back-donation (Scheme 2).

With the charge differences on the N<sub>2</sub> groups of X-1 being rather similar, the question becomes pertinent as to how the positive charge is distributed in the XPh fragment. Chemical intuition might be guided by the directing effects of the diazonium function in electrophilic and nucleophilic aromatic substitutions and N<sub>2</sub> displacement chemistry.<sup>38</sup> Benzenediazonium ions are susceptible to electrophilic attack at the *meta* position and to nucleophilic attack on the terminal nitrogen<sup>39</sup> and at the *ortho* and *para* positions of the aromatic ring.<sup>40</sup> Hence, one would be inclined to assume that the diazonium substituent causes electron density depletion at the *ortho* and *para* positions as indicated by the formal charges of resonance forms B–D. The charges on the *ortho*, *meta*, and *para* carbons are all very small ( $|q(\text{C})| < 0.08$ ), and most of the positive charge resides on the hydrogens. Comparison of the CH group charges does not indicate larger depletions of electron density at the *ortho* and *para* positions, but instead, the charges of C atom and CH group (*ortho* 0.190, *meta* 0.166, *para* 0.124) decrease with increased distance from the N<sub>2</sub> substituent.

In H-1, the H<sub>para</sub> atom acts just like the other aromatic hydrogens to delocalize positive charge to the periphery of the molecule while the X groups are negatively charged in NH<sub>2</sub>-1 and NO<sub>2</sub>-1. The NH<sub>2</sub> group overall withdraws 0.475 electrons while  $\pi$ -donating 0.156 electrons! The NO<sub>2</sub> group overall withdraws 0.531 electrons, and 0.063 of that is due to  $\pi$ -withdrawal. The effects of the substitution are best discussed considering the charge differences of X-1 relative to H-1 shown on the bottom of Figure 5. For example, the value  $\Delta q(\text{NH}_2) = 0.581$  is the difference between the charge of H<sub>para</sub> in H-1 and the NH<sub>2</sub> group in NH<sub>2</sub>-1,  $\Delta q = q(\text{X-1}) - q(\text{H-1})$ , and changes of  $\pi$ -charges were computed in a similar fashion. With the negative charge accumulation on the NH<sub>2</sub> group ( $\Delta q < 0$ ) comes a build-up of positive charge on  $C_{\text{para}}$  which exceeds the electron density build-up on the NH<sub>2</sub> group in magnitude. Evidently it is electrostatically beneficial

(38) (a) Replacement by F<sup>-</sup>, for a review, see: Suschitzky, H. *Adv. Fluorine Chem.* **1965**, 4, 1. (b) Replacement by OH<sup>-</sup>: Dreher, E.-L.; Niederer, P.; Rieker, A.; Schwarz, W.; Zollinger, H. *Helv. Chim. Acta* **1981**, 64, 488.

(39) Examples of nucleophilic attack include: (a) Haub, E. K.; Lizano, A. C.; Noble, M. E. *J. Am. Chem. Soc.* **1992**, 114, 2218. (b) Carroll, J. A.; Fisher, D. R.; Canham, G. W. R.; Sutton, D. *Can. J. Chem.* **1974**, 52, 1914. (c) Einstein, F. W. B.; Sutton, D.; Vogel, P. L. *Can. J. Chem.* **1978**, 56, 891.

(40) (a) Lewis, E. S.; Johnson, M. D. *J. Am. Chem. Soc.* **1960**, 82, 5399. (b) Lewis, E. S.; Johnson, M. D. *J. Am. Chem. Soc.* **1960**, 82, 5408. (c) Lewis, E. S.; Chalmers, D. J. *J. Am. Chem. Soc.* **1971**, 93, 3267.

(37) For the parent system, a similar behavior was found at the MP2(full)/6-31G\* level along the dissociation paths and  $Q$  values derived from the MP2 structures X-1 and X-2 show the same trends.

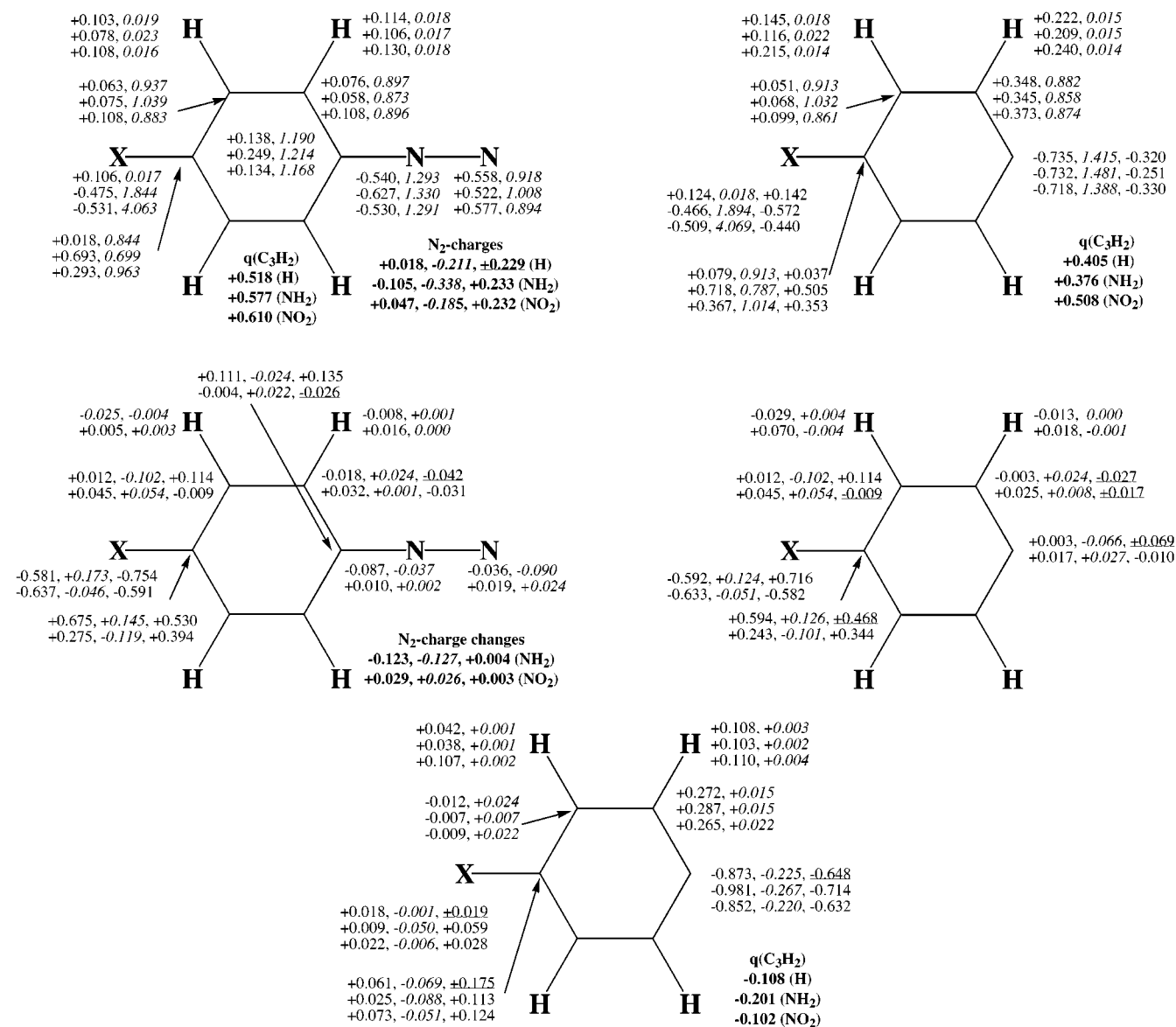


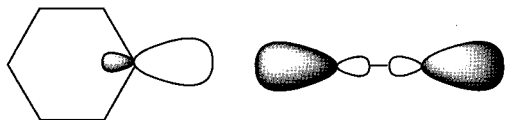
**Figure 5.** Integrated atom and fragment charges and populations as determined with the RHF/6-31G\* densities of X-1 and X-2. The  $\pi$ -populations are given in italics and  $\sigma$ -charges are the third values. The data on the top right specify the changes associated with dediazonation. The data on the bottom are relative to H-1 or H-2.

to locate as much positive charge as possible right next to the negative NH<sub>2</sub> group. While the NH<sub>2</sub> group is an electron acceptor, it is the H<sub>2</sub>N–C<sub>para</sub> fragment that acts as a donor. It is for this reason that electron density gains occur on all CH groups but the overall electron density of the C<sub>ipso</sub>–N<sub>2</sub> fragment is increased very little, only 0.013 electrons! The  $\pi - \Delta q$  values of the NH<sub>2</sub> group and of C<sub>para</sub> both are positive and combine to a  $\pi$ -donation of 0.318 with the main beneficiary being C<sub>ipso</sub> and the N<sub>2</sub> group with a gain of 0.151 electrons. Thus, these electron density shifts do show the enhanced C  $\rightarrow$  N  $\pi$ -backdative bonding in NH<sub>2</sub>-1 but the actual electronic origin is much more complex than the simplistic  $\pi$ -pushing picture and, in particular, these electron density shifts leave the amino group very negative. The  $\sigma$ -density of the N<sub>2</sub> group is changed little but C<sub>ipso</sub> is depleted in  $\sigma$ -density, and these events are expected to strengthen the N  $\rightarrow$  C  $\sigma$ -dative bonding in NH<sub>2</sub>-1. Both components of the CN interaction are thus enhanced in NH<sub>2</sub>-1. The NO<sub>2</sub> group acts different in that the build-up of positive charge at C<sub>para</sub> is much less than the negative charge on the NO<sub>2</sub>

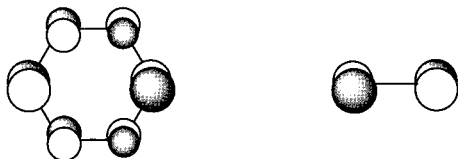
group and positive charge increases occur at the *o*-CH groups, at C<sub>meta</sub>, and at the N<sub>2</sub> group. The C<sub>para</sub> atom in NO<sub>2</sub>-1 is entirely different from C<sub>para</sub> in NH<sub>2</sub>-1 in that it is placed next to an overall positive atom of the NO<sub>2</sub> group. Electrostatic attractions between C<sub>para</sub> and the nitro O atoms are counteracted by electrostatic C<sub>para</sub>–N repulsion. The C<sub>ipso</sub>–N<sub>2</sub> fragment overall loses 0.025 electrons compared to H-1. The  $\pi - \Delta q$  values of the nitro group and of C<sub>para</sub> both are negative and combine to a  $\pi$ -withdrawal of 0.165 causing depletions of  $\pi$ -density at C<sub>meta</sub>, C<sub>ipso</sub>, and N <sub>$\beta$</sub> . The overall charge changes of the N<sub>2</sub> group are thus very similar to the changes in the  $\pi$ -system. These electron density shifts suggest that the NO<sub>2</sub> group hardly affects N  $\rightarrow$  C  $\sigma$ -dative bonding but weakens C  $\rightarrow$  N  $\pi$ -backdative bonding.

The results of the density analysis perfectly explain the structural trends in X-1. Our analysis suggests enhanced CN bonding in NH<sub>2</sub>-1 and weakened CN bonding in NO<sub>2</sub>-2, and the CN bond lengths in X-1 are consistent with this trend. Moreover, the NN bond length in NH<sub>2</sub>-1 is lengthened noticeably compared to H-1 and

**Scheme 2. Primary MO Interactions Associated with  $\sigma$ -Dative  $N \rightarrow C$  and  $\pi$ -Backdative  $C \rightarrow N$  Bonding in Benzenediazonium Ions**



$\sigma$ -donor interaction between the  $N_2$  lone pair and the vacant  $\sigma$ -orbital on phenyl cation.



$\pi$ -backdative bonding involves a  $\pi$ -orbital of phenyl cation and the  $\pi^*$  orbital of  $N_2$ .

$NO_2$ -1. It has long been known that NN bond lengths in diazonium ions are shorter than those in free  $N_2$ .<sup>41</sup> This feature is inconsistent with severe electron depletion of the  $N_2$  group, but it is explained by the electron density analysis as the result of increased N–N bond polarity. Another prominent feature of X-1 concerns the  $C_{ipso}$  ring angle.<sup>42</sup> The angles in the phenyl ring are sensitive to the nature of attached substituents. It is thought that substituents that deplete  $C_{ipso}$  of electron density exert an angle-widening effect to increase this C atom's s-character.<sup>43</sup> In the extreme case of the phenyl cation,<sup>44</sup> the ring angle at  $C_{ipso}$  is widened to 146.9°. H-1 and  $NO_2$ -1 both show a small but substantial widening (125.1°) of the angle at the positively charged  $C_{ipso}$  atom (0.138 and 0.134). It should be noted, however, that the angle–charge relation is too simplistic as is evident from the data for  $NH_2$ -1. Clearly, an angle widening at  $C_{ipso}$  is beneficial to the Coulombic term at  $C_{ipso}$  but, at the same time, such an angle-widening would reduce the exchange interactions associated with dative CN bonding and our discussion shows the latter to be more important in  $NH_2$ -1 than in H-1 and  $NO_2$ -1.

**Electronic Structure of Phenyl Cations.** The population analysis of H-2 assigns a negative charge to  $C_{ipso}$

(41) This feature is common to aromatic and aliphatic diazonium ion. Compare the discussion in ref 5b.

(42) For a detailed discussion, see: Horan, C. J.; Barnes, C. L.; Glaser, R. *Chem. Ber.* **1993**, *126*, 243.

(43) (a) Bock, H.; Ruppert, K.; Näther, C.; Havlas, Z.; Herrmann, H.-F.; Arad, C.; Göbel, I.; John, A.; Meuret, J.; Nick, S.; Rauschenbach, A.; Seitz, W.; Vaupel, T.; Solouki, B. *Angew. Chem., Int. Ed. Engl.* **1992**, *31*, 550. (b) Domenicano, A.; Vaciano, A.; Coulson, C. A. *Acta Crystallogr.* **1975**, *B31*, 221. (c) Domenicano, A.; Vaciano, A.; Coulson, C. A. *Acta Crystallogr.* **1975**, *B31*, 1630. (d) Domenicano, A.; Vaciano, A. *Acta Crystallogr.* **1979**, *B35*, 1382. (e) Domenicano, A.; Murray-Rust, P.; Vaciano, A. A. *Acta Crystallogr.* **1983**, *B39*, 457. (f) Domenicano, A. *Structural Substituent Effects in Benzene Derivatives*. In *Accurate Molecular Structures—Their Determination and Importance*; Domenico, A., Hargittai, I., Eds.; IUCr/Oxford University Press: 1992.

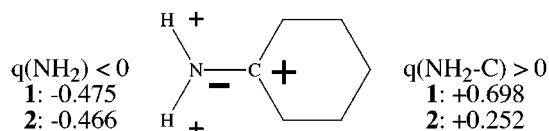
(44) For prior ab initio calculations of phenyl cation, see: (a) Dill, J. D.; Schleyer, P. v. R.; Binkley, J. S.; Seeger, R.; Pople, J. A.; Haselbach, E. *J. Am. Chem. Soc.* **1976**, *98*, 5428. (b) Dill, J. D.; Schleyer, P. v. R.; Pople, J. A. *J. Am. Chem. Soc.* **1977**, *99*, 1. (c) Schleyer, P. v. R.; Kos, A. J.; Raghavachari, K. *J. Chem. Soc., Chem Commun.* **1983**, 1296. (d) Krogh-Jespersen, K.; Chandrasekhar, J.; Schleyer, P. v. R. *J. Org. Chem.* **1980**, *45*, 1608. (e) Apeloig, Y.; Arad, D. *J. Am. Chem. Soc.* **1985**, *107*, 5285. (f) Uggerud, E.; Arad, D.; Apeloig, Y.; Schwarz, H. *J. Chem. Soc., Chem Commun.* **1989**, 1015. (g) Tasaka, M.; Ogata, M.; Ichikawa, H. *J. Am. Chem. Soc.* **1981**, *103*, 1885. (h) Bernardi, F.; Grandinetti, F.; Guarino, A.; Robb, M. A. *Chem. Phys. Lett.* **1988**, *153*, 309.

at all theoretical levels, and the  $o$ -CH groups carry large positive charges. These populations reflect the polarizations of the  $C_{ipso}$ – $C_{ortho}$  bonds toward  $C_{ipso}$ . The bond critical points of the  $C_{ipso}$ – $C_{ortho}$  bonds move significantly further away from  $C_{ipso}$  in going from H-1 to H-2 and the atomic basin of  $C_{ipso}$  grows. We will focus on the population of the  $C_3H_2$  fragment as a whole and note that its overall positive charge is greatly diminished (by 0.108) during dediazonation. The  $\sigma$ -hole formation causes such extreme polarizations in the  $\sigma$ -system that the larger part of the positive charge is located in the other half of the molecule! The phenyl ring gains  $\pi$ -density upon dediazonation, and this density largely remains located at  $C_{ipso}$ . The charge density relaxation associated with dediazonation of  $NO_2$ -1 is quite similar. It follows that the dediazonation of  $NO_2$ -1 places positive charge into the region that was already more deplete of electron density to begin with because of the  $NO_2$  group's electron withdrawal. We argue that it is this feature of the internal charge transfer in  $NO_2$ -2 that causes the dissociation of  $NO_2$ -1 to be more endothermic than that of H-1. The  $NH_2$ -2 ion has by far the lowest positive charge on the  $C_3H_2$  fragment (+0.376), and the reduction of positive charge on this fragment upon dediazonation also is by far the highest (–0.201). This increase in electron density is due in part to the departure of the  $N_2$  group leaving behind 0.105 electrons and increases in positive charge on  $H_{meta}$  and  $C_{para}$ . The charge increases in the X-substituted half of the molecule are generally smaller as compared to those of H-1 and  $NO_2$ -2. Interestingly, the dediazonation is accompanied by a decrease of the  $\pi$ -donation from the  $H_2N$ – $C_{para}$  fragment; the  $\sigma$ -polarizations in  $NH_2$ -2 are so effective that the  $\pi$ -donation actually is reduced. All features of these electronic properties would suggest that amino substitution of the phenyl cation should lead to thermodynamic stabilization. It thus appears that the higher binding energy for  $NH_2$ -1 reflects primarily the stronger CN bonding providing thermodynamic stabilization in the push–pull stabilized diazonium ion.

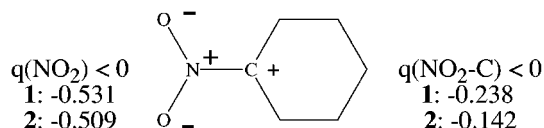
**Mode of Action of the Amino and the Nitro Groups.** The proposition that the amino group is an overall electron-withdrawing group often runs into opposition. Amino groups clearly *function* as electron-donating groups, and it is still commonly thought that the source of the electron donation consists of the charge transfer associated with the displacement of N lone pair electron density. Our discussion shows that it is perfectly compatible for the amino group to *function* as an electron donor and while it is negatively charged at the same time. This is illustrated in Scheme 3 for both 1 and 2. The amino group withdraws electron density from the H-atoms and from the phenyl ring. The charge built-up at the C-atom to which the amino group is attached exceeds the charge of the benzene ring, and it is the reservoir of electron density. The function of the amino group as an electron donor is thus the result of the amino group's ability to induce strong polarization. The overall charge of the amino and nitro groups is not all that different ( $-0.50 \pm 0.05$ ), but the charge distribution within the two substituents is drastically different. With the nitro N-atom having a positive charge, the induced polarization of the positively charged benzene ring will be such as to minimize the positive charge on the C-atom that carried the nitro group. While  $q(NH_2)$  and  $q(NO_2)$  both are

**Scheme 3. Mode of Action of the Amino and the Nitro Groups. While  $q(\text{NH}_2)$  and  $q(\text{NO}_2)$  Are Both Negative,  $q(\text{NH}_2\text{-C})$  and  $q(\text{NO}_2\text{-C})$  Drastically Differ in That the Former Is Positive and the Latter Is Negative**

C-atom attached to NH<sub>2</sub> group is in favorable environment to assume large positive charge.



C-atom attached to NO<sub>2</sub> group is not in favorable environment to assume large positive charge.



negative,  $q(\text{NH}_2\text{-C})$  and  $q(\text{NO}_2\text{-C})$  drastically differ in that the former is positive and the latter is negative.

**Electronic Relaxation along the Dediazonium Path.** The plots in Figure 6 depict the progression of the charges and of the atom dipole moments of the N-atoms of H-1 as the CN distance increases. At a distance of 3.0 Å, the dissociation is essentially complete and the complex consists of H-2 and neutral and nearly unpolarized N<sub>2</sub>. The charges of N<sub>α</sub> and N<sub>β</sub> change rather steadily, and their dipole moments increase until they are of equal magnitude and antiparallel. The negative charge on N<sub>α</sub> drops faster than the positive charge on N<sub>β</sub>, and thus, the N<sub>2</sub> group charge goes through a maximum around 1.8 Å. These trends in the electronic relaxation of H-1 are the same at the levels RHF/6-31G\* and MP2(full)/6-31G\*. In Figure 7, the CN distance dependencies of the electronic relaxations of X-1 are compared. Dediazonation always involves a nonmonotonic change of the total N<sub>2</sub> group charge. Irrespective of the N<sub>2</sub> group charge in the equilibrium structure X-1, the N<sub>2</sub> group charge does become positive in the early phase of the dissociation, it reaches a maximum charge of 0.1 and 0.2, and then it smoothly turns neutral in the later stages of the dissociation. The value of  $q_{\text{max}}(\text{N}_2)$  of the *p*-nitro-substituted system exceeds  $q_{\text{max}}(\text{N}_2)$  of the parent, and  $q_{\text{max}}(\text{N}_2)$  of the *p*-amino-substituted ion is the lowest. All three molecules go through the maximum at a C–N distance of about 1.75 Å. The N<sub>2</sub>  $\pi$ -population quickly and steadily decreases with increasing C–N distance while the  $\sigma$ -population component decreases and approaches zero at a slower rate. Our analysis shows in a compelling fashion that the C → N  $\pi$ -backdative bond breaks earlier than the N → C  $\sigma$ -dative bond.

**CN Bonding Model and Opposing Sign Reaction Constants in DSP Relations.** Dediazoniations are prominent representatives of the group of only 16 reactions for which dual substituent parameter (DSP) treatments result in *opposing* signs of the reaction constants  $\rho_F$  and  $\rho_R$ . Taft analysis of dediazoniations of substituted benzenediazonium ions yields reactions constants  $\rho_F < -3.5$ ,  $\rho_R > +2.2$ , and  $|\rho_F| > |\rho_R|$  and evoked the following interpretations. For the dissociations X-1 → X-2 + N<sub>2</sub>,

the cleavage of the  $\sigma$ -dative bond between the N<sub>2</sub> lone pair and the sp<sup>2</sup> LUMO of 2 is slowed by inductively withdrawing substituents and should give rise to a negative field reaction constant  $\rho_F$ . If  $\sigma$ -dative N → C bonding is reinforced by C → N  $\pi$ -backdative bonding, then one can argue that a positive reaction constant  $\rho_R$  is plausible since dissociation leads to an increase of  $\pi$ -density accumulation on the phenyl fragment and brings  $\pi$ -electron density closer to the substituent. A rationalization of the relation  $|\rho_F| > |\rho_R|$  would be much more difficult because energetic consequences of charge shifts in the  $\sigma$ - and  $\pi$ -frames are not amenable to simple estimation.

The theoretical results presented here support the earlier interpretation and show it to be consistent with the electron density based model that describes CN bonding in benzenediazonium ions by synergistic  $\sigma$ -dative C ← N and C → N  $\pi$ -backdative bonding. Moreover, the theoretical analysis provides details about the electronic structure that cannot be deduced from physical-organic studies alone. The kinetic analysis provides information about the direction of charge shifts but does not quantify beyond simple considerations of the magnitudes of the reaction constant(s). For example, the results of the kinetic analysis do not answer the question as to whether the negative reaction constant  $\rho_F$  is due to positive charge being transferred from the diazo function onto the phenyl fragment (e.g., Lewis notation) or whether it is merely the result of charge shifts within the phenyl fragment (as we show). Only the analysis of the electron density distributions in Cartesian space reveals that CN bonding in diazonium ions occurs with only a very small amount of overall charge transfer between phenyl cation and N<sub>2</sub>. The CN bonding is achieved via  $\sigma$ -dative C ← N and C → N  $\pi$ -backdative bonding components of nearly equal magnitude and either one may dominate. For the linear unimolecular dissociation, the cleavage of the CN bond may increase (X = H, NO<sub>2</sub>) or decrease (X = NH<sub>2</sub>) the overall positive charge on the phenyl fragment. However, in all of these cases CN dissociation leads to a steady increase of positive charge in the  $\sigma$ -system and a steady increase of  $\pi$ -density on the phenyl fragment.

The kinetic analysis makes statements about substituent effects on the overall energy changes between reagents and products which then form the basis for deductions as to stabilization mechanisms operating in either one of these. The theoretical analysis allows one to pinpoint such stabilization mechanisms since it provides independent information about reagents and products and we thus can examine the electronic reasons for the ordering  $E_b(\text{X} = \text{NH}_2) > E_b(\text{X} = \text{NO}_2) > E_b(\text{X} = \text{H})$ . The dogmatic interpretation would focus on substituent effects on phenyl cation and argue that one might have expected the opposite since the nitro group is more electron withdrawing than the amino group and, in addition, because the  $\pi$ -donor might better compensate the electron deficiency in the  $\sigma$ -frame via polarization of the  $\pi$ -system. This analysis then demands some mechanism to provide an extra stabilization to NH<sub>2</sub>-1 as compared to NO<sub>2</sub>-1 and leads to the idea of push–pull stabilization of spacer-connected  $\pi$ -donor–acceptor systems. Our density analysis confirms an extra stabilization of NH<sub>2</sub>-1 over NO<sub>2</sub>-1 but also reveals features in the electronic structures that do differ significantly from expectations. These electron density shifts manifest enhanced C → N  $\pi$ -backdative bonding in NH<sub>2</sub>-1, but the

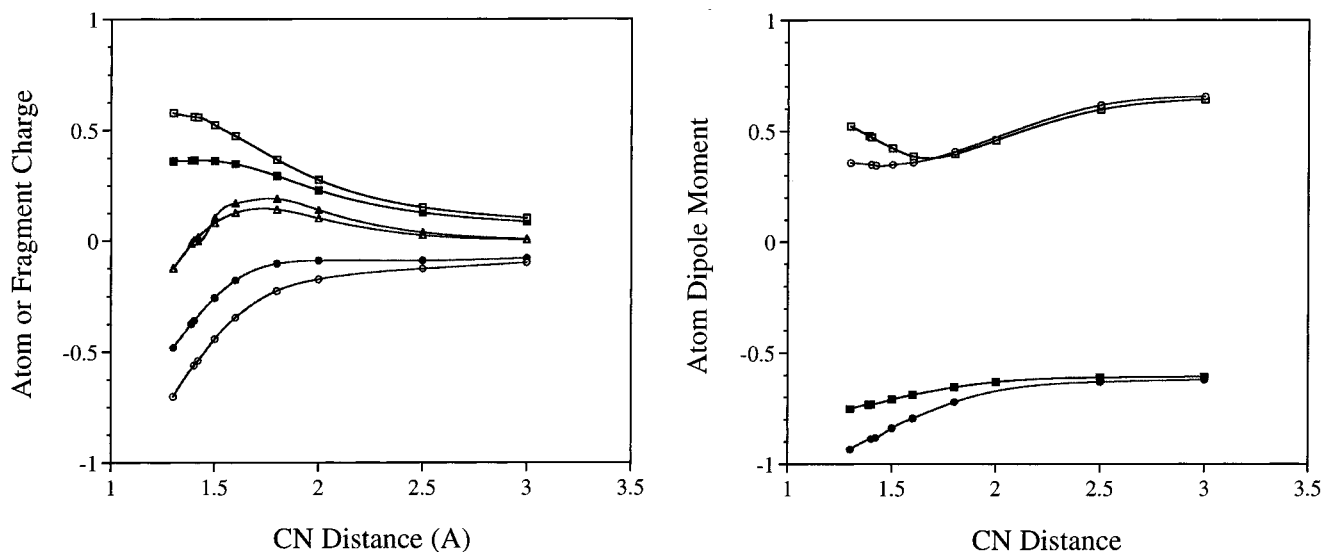


**Figure 6.** Variations of the atomic charges and dipole moments of the N-atoms along the dissociation path H-1 to H-2 and N<sub>2</sub>. Data for N<sub>α</sub> (circles), N<sub>β</sub> (squares), and N<sub>2</sub> group (triangles) were computed at the RHF/6-31G\* (unfilled) and MP2(full)/6-31G\* (filled) levels.

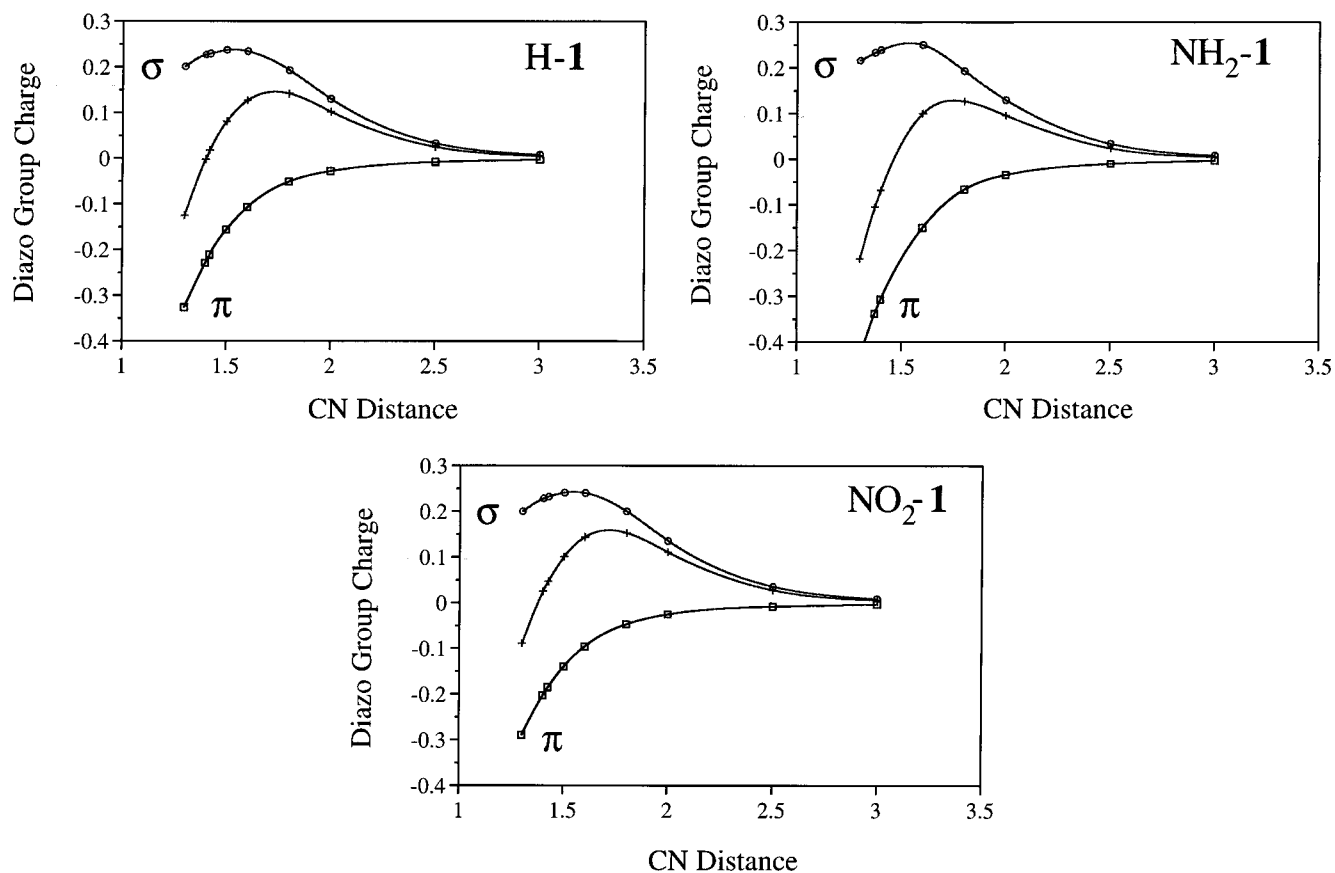


**Figure 7.** Total N<sub>2</sub> group charge  $q(N_2)$  and components  $q(\sigma)$  and  $q(\pi)$  as a function of the CN distance along a unimolecular dediazonation paths of H-1, NH<sub>2</sub>-1, and NO<sub>2</sub>-1.

actual electronic structure is much more complex than the simplistic  $\pi$ -pushing picture and leaves the amino group very negative. Rather counter-intuitive also are the electron-density shifts in NO<sub>2</sub>-1 as they show that the NO<sub>2</sub> group hardly affects N  $\rightarrow$  C  $\sigma$ -dative bonding but weakens C  $\rightarrow$  N  $\pi$ -backdative bonding. Note that our electron density analysis suggests enhanced CN bonding in NH<sub>2</sub>-1 and weakened CN bonding in NO<sub>2</sub>-1 and it is perfectly consistent with the structural trends in X-1. As

to the phenyl cations X-2, extreme polarizations in the  $\sigma$ -systems cause the larger part of the positive charge to be located not on the C<sub>3</sub>H<sub>2</sub> fragment but in the other half of the molecule! The positive charge of the C<sub>3</sub>H<sub>2</sub> fragment is greatly diminished ( $> 0.1$  e) during dediazonation and moved into the X-substituted region. Even though the overall charge of the phenyl fragments in 1 and 2 differ relatively little, there clearly is a pronounced shift of electron density away from X and it is this shift that we

consider responsible for the negative reaction constant  $\rho_F$ . The phenyl ring gains  $\pi$ -density upon dediazonation which is consistent with the positive reaction constant  $\rho_R$ . Interestingly, the  $\sigma$ -polarizations in NH<sub>2</sub>-**2** are so effective that the  $\pi$ -donation actually is reduced compared to that of NH<sub>2</sub>-**1**. The density analysis shows that dediazonation of NO<sub>2</sub>-**1** places positive charge into the region that was already more deplete of electron density to begin with because of the NO<sub>2</sub> groups electron withdrawal. We argue that it is this feature of the internal charge transfer in NO<sub>2</sub>-**2** that causes the dissociation of NO<sub>2</sub>-**1** to be more endothermic than that of H-**1**. On the other hand, the electron density analysis indicates that amino substitution of phenyl cation should lead to thermodynamic stabilization and suggests that the higher binding energy for NH<sub>2</sub>-**1** reflects primarily the stronger CN bonding in the push–pull stabilized benzenediazonium ion.

### Conclusion

The detailed analysis of a selection of systems with counteracting effects in the  $\pi$ - and  $\sigma$ -systems demonstrates that the classical tool of  $\pi$ -electron pushing does not suffice to provide a correct account of the electronic structures. This conclusion is significant as it affects the way we ought to think of the majority of donor–acceptor substituted conjugated dyes and nonlinear optical materials. This important point also has been exemplified

recently by our electronic structure analysis of the nonlinear optical (NLO) materials NPO (4-nitropyridine *N*-oxide) and POM (3-methyl-NPO).<sup>45</sup> Polarizations in the  $\sigma$ -frames critically affect structures ( $Q$  values) and electronic structures (populations) and consistent explanations of structural and energetic relaxations in the course of reactions require their explicit consideration. This result also has significant implications with regard to all other reactions in which  $\sigma$ - and  $\pi$ -polarizations act in concert ( $\lambda$  positive). If  $\sigma$ -polarizations dominate in cases where they counteract  $\pi$ -effects, it would seem reasonable to assume that they also are of comparable magnitude in cases where  $\sigma$ - and  $\pi$ -effects act in concert. In the later case, explanations based on  $\pi$ -polarizations might therefore seem consistent but they might lack a physical basis.

**Acknowledgment.** The research was supported by grants from the Research Council and the Research Board of the University of Missouri. M.L. thanks the Natural Sciences and Engineering Research Council (NSERC) of Canada for a Postgraduate Scholarship Type A.

**Supporting Information Available:** Topological and integrated properties of the stationary structures X-**1** and X-**2**. This material is available free of charge via the Internet at <http://pubs.acs.org>.

JO9818430

---

(45) Glaser, R.; Chen, G. S. *Chem. Mater.* **1997**, *9*, 28.